

# Homogeneous Oxidation Reactions of Propanediols at Low Temperatures

Eva Díaz,<sup>[a, b]</sup> María Eugenia Sad,<sup>[a, c]</sup> and Enrique Iglesia<sup>\*[a]</sup>

O<sub>2</sub> reacts with propanediols via homogeneous pathways at 400–500 K. 1,2-Propanediol forms CH<sub>3</sub>CHO, HCHO, and CO<sub>2</sub> via oxidative C–C cleavage and acetone via dehydration routes, while symmetrical 1,3-propanediol undergoes dehydration and oxidative dehydrogenation to form, almost exclusively, acrolein (ca. 90% selectivity). The products formed and their kinetic dependence on reactant concentrations are consistent with radical-mediated pathways initiated by O<sub>2</sub> insertion into C–H bonds in a β position relative to oxygen atoms in diol reac-

tants. Propagation involves β-scission reactions that form hydroxyl and hydroxyalkyl radicals. Acrolein/O<sub>2</sub>/H<sub>2</sub>O mixtures from the homogeneous oxidation of 1,3-propanediol form acrylic acid (with 90% yield) in tandem reactors containing molybdenum-vanadium oxide catalysts. These data reveal the unique reactivity of diols, compared with triols and alkanols, in homogeneous oxidations, while also providing useful insight into the molecular basis for reactivity in biomass-derived oxygenates.

## Introduction

The conversion of biomass-derived feedstocks to liquid fuels remains a formidable challenge.<sup>[1–5]</sup> Transesterification of triglycerides in biodiesel production leads to glycerol as a low-cost byproduct,<sup>[6]</sup> making routes for its subsequent chemical conversion attractive. Glycerol can be converted into 1,3-propanediol by either enzymatic dehydration and subsequent reduction, or via deoxygenation.<sup>[7]</sup> 1,2-Propanediol can be produced from glycerol via reactive distillation using copper chromite catalysts.<sup>[4]</sup> Several studies have addressed the pyrolysis, dehydration, etherification, esterification, and reforming reactions of glycerol, as well as its oxidative conversion; the latter paths include oxidation at terminal OH groups to form glyceric and tartaric acids, at secondary OH groups to give hydroxyacetone, and at all OH groups to form ketomalonic or mesoxalic acids.<sup>[4,8]</sup> Markets for such products remain immature, at least in part because these oxidations exhibit low selectivities and yields and involve inefficient liquid-phase processes using dilute aqueous glycerol. The multifunctional nature of triols and the concomitantly diverse conversion pathways and products lead, in general, to poor selectivities.<sup>[3]</sup>

Reactions of diols derived from glycerol have also been studied, albeit less thoroughly. 1,2-Propanediol reacts with O<sub>2</sub> to form hydroxyacetone as the initial product and methylglyoxal via subsequent oxidation of hydroxyacetone on Ag catalysts (500–700 K).<sup>[9,10]</sup> Methylglyoxal selectivities decrease with increasing conversion, because of sequential oxidation and cracking reactions. In electrochemical processes catalyzed by Au and Pt,<sup>[11–13]</sup> 1,2-propanediol oxidation led to the predominant cleavage of C–C bonds, while 1,3-propanediol preferentially formed hydroxypropanoic acid via routes analogous to those involved in oxidation of primary alkanols.

Here, we show that 1,2 and 1,3-propanediols react with O<sub>2</sub> via previously unreported homogeneous gas-phase routes at modest temperatures (400–600 K). 1,3-Propanediol gives acro-

lein selectivities of ca. 90% at 430 K. 1,2-Propanediol forms acetone (ca. 25% selectivity) and also decomposes into acetaldehyde, formaldehyde, and CO<sub>2</sub> via C–C cleavage. Rates were strictly proportional to the reactor volume and unaffected by contact with heated transfer lines or other surfaces, consistent with exclusively homogeneous pathways. The effects of propanediol and O<sub>2</sub> pressures on oxidation rates and the identity of the products formed are consistent with chain propagation processes mediated by oxygen-containing radicals.

The high acrolein selectivity in homogeneous 1,3-propanediol oxidation led us to introduce the acrolein and H<sub>2</sub>O formed together with unreacted O<sub>2</sub> into a second reactor containing a Mo–V oxide catalyst,<sup>[14]</sup> able to convert acrolein into acrylic acid with 90% yields (based on propanediol reactants). This combined process provides a route for concurrent oxidation of difficult-to-separate 1,2 and 1,3-propanediols, formed via glycerol hydrogenolysis, into useful products (acrylic and acetic acids, acetone, acetaldehyde). This study also provides a kinetic framework relevant to the practice of these chemistries, as well as mechanistic insights into homogeneous pathways for the

[a] Dr. E. Díaz, Dr. M. E. Sad, Prof. E. Iglesia  
Department of Chemical Engineering, University of California at Berkeley  
Berkeley, CA 94720 (USA)  
Fax: (+1) 510-642-4778  
E-mail: iglesias@berkeley.edu

[b] Dr. E. Díaz  
Department of Chemical and Environmental Engineering  
University of Oviedo  
C/Julian Claveria, s/n, 33006 Oviedo (Spain)

[c] Dr. M. E. Sad  
UNL CONICET, Inst Invest Catalisis & Petroquim INCAPE, GICIC  
RA-3000 Santa Fe (Argentina)

Supporting Information for this article is available on the WWW under <http://dx.doi.org/10.1002/cssc.201000142>.

oxidative activation of chemical bonds in typical biomass-derived oxygenates.

## Results and Discussion

### Homogeneous 1,3-propanediol oxidation

Rates, conversions, and selectivities for the gas-phase oxidation of 1,3-propanediol at 400–600 K and 12.4 s residence time are shown in Figure 1. No products were detected in the absence of  $O_2$ . The absence of surface-mediated conversion pathways was confirmed by displacing the reactor volume with glass beads (6.5–9.0  $cm^3$  volume) at constant residence time and 430–570 K.

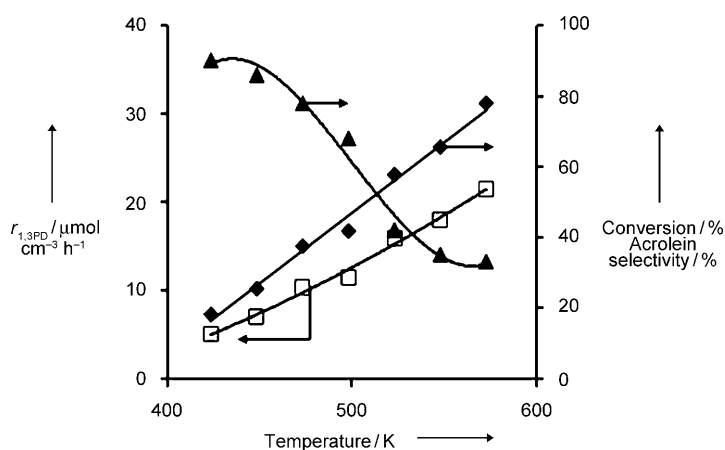


**Figure 1.** 1,3-Propanediol conversion ( $\blacklozenge$ ), oxidation rate ( $\square$ ), and acrolein selectivity ( $\blacktriangle$ ) as a function of temperature (12.4 s residence time; residence time is defined as the reactor volume divided by the total volumetric (STP) flow rate; 0.47 kPa  $O_2$ , 0.28 kPa 1,3-propanediol).

Conversion rates and selectivities were independent of reactor volume for a given residence time (Figure 2). Reactant conversions and selectivities were not influenced by changes in the temperature of the transfer lines before or after the reactor and conversion products were not detected when the reactor

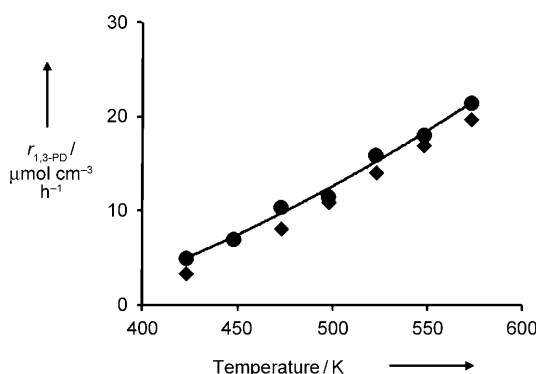


**Figure 2.** Comparison of reaction rates obtained for oxidation at a space time of 12.4 s and two different reactor volumes: 6.5 ( $\blacklozenge$ ) and 9  $cm^3$  ( $\bullet$ ); 0.47 kPa  $O_2$ , 0.28 kPa 1,3-propanediol).

vessel was bypassed. We conclude from these data that propanediol oxidation products formed only within the heated vessel at rates proportional to its volume and without contributions from surface-mediated radical initiation or termination reactions.

Alkanols (e.g., 1-propanol and 2-propanol) reacted with  $O_2$  only at significantly higher temperatures than diols (700 K, vs. 400–500 K) and predominantly formed  $CH_4$  and  $CO_x$ .<sup>[15]</sup> Glycerol did not react with  $O_2$  at the temperatures of this study (430–570 K), as also reported in previous studies.<sup>[16]</sup> Thus, the homogeneous pathways reported here appear to reflect a reactivity in radical-mediated pathways that appears to be unique to diols among  $C_3$  oxygenates.

Figure 1 shows that acrolein was the predominant product formed at low temperatures (< 500 K); acrolein selectivities decreased with increasing temperature (Figure 1), while acetaldehyde and formaldehyde selectivities concurrently increased (Table 1).  $CO$  was not detected in the reactor effluent (< 0.2% selectivity) and  $CO_2$  selectivities were less than 2%. These high selectivities to a single product (ca. 90% acrolein, 400–450 K) are unusual in homogeneous oxidations, which typically form a wide range of products because of the unselective nature of C–H bond activation steps involved in chain initiation and propagation steps. High acrolein selectivities were maintained even as diol reactants reached nearly complete conversion with increasing residence time (91% selectivity at > 99% conversion; 543 K, 8.8 kPa  $O_2$ , 1 kPa diol, 14.1 s residence time).

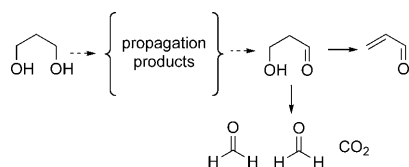
1,3-Propanediol oxidation pathways were probed by measuring the effects of residence time on product selectivities (Table 1). Selectivities were independent of residence time, consistent with the products

**Table 1.** Conversion, reaction rate, and selectivity towards acrolein, acetaldehyde, and formaldehyde in the oxidation of 1,3-propanediol, as function of residence time.<sup>[a]</sup>

$\tau$ [s]	Conversion [%]	$-r_{1,3PD}$ [ $\mu\text{mol cm}^{-3} \text{h}^{-1}$ ]	Selectivity [%]			
			Acrolein	$CH_3CHO$	HCHO	$CO_2$
18.6	32.9	10.2	90	6.0	1.8	2.0
11.9	23.1	10.7	91	6.8	2.0	0.2
9.6	20.0	12.4	93	5.5	1.3	0.2
7.4	12.0	9.3	92	6.1	1.7	0.2
6.0	8.8	8.1	89	8.2	1.6	1.0
8.9 <sup>[b]</sup>	11.8	9.6	93	4.6	0.9	1.3
12.4 <sup>[c]</sup>	23.1	10.9	90	6.4	1.3	2.0

[a] Conditions:  $T = 430$  K, 0.28 kPa 1,3-propanediol, 0.89 kPa  $O_2$ . [b] Varied by changing the reactor volume from 9 to 6.5  $cm^3$  by displacement with quartz beads. [c] Interpolated from the above data to allow comparisons at identical reactant conversions.  $\tau$  is the residence time, defined as the ratio between the reactor volume and the volumetric flow rate at inlet conditions.

formation as primary products from 1,3-propanediol via parallel direct pathways (Scheme 1) and with their inertness in secondary oxidations. The  $CH_3CHO/(HCHO+CO_2)$  molar ratios in



**Scheme 1.** Homogeneous oxidation pathways of 1,3-propanediol.

products were near unity and unaffected by residence time, consistent with C<sub>1</sub> and C<sub>2</sub> species that form concurrently via C–C bond cleavage from diol-derived species. The ratio of CO<sub>2</sub>/HCHO varied from 0.1 to 1.5, apparently because of secondary decomposition of HCHO to CO<sub>x</sub>. The addition of acrolein to 1,3-propanediol/O<sub>2</sub> reactants did not influence the effluent composition or the diol conversion rate or selectivity.

The effects of 1,3-propanediol and O<sub>2</sub> reactant pressures on acrolein and acetaldehyde formation rates (430 K) are shown in Figures 3 and 4. Acrolein formation rates increased with in-

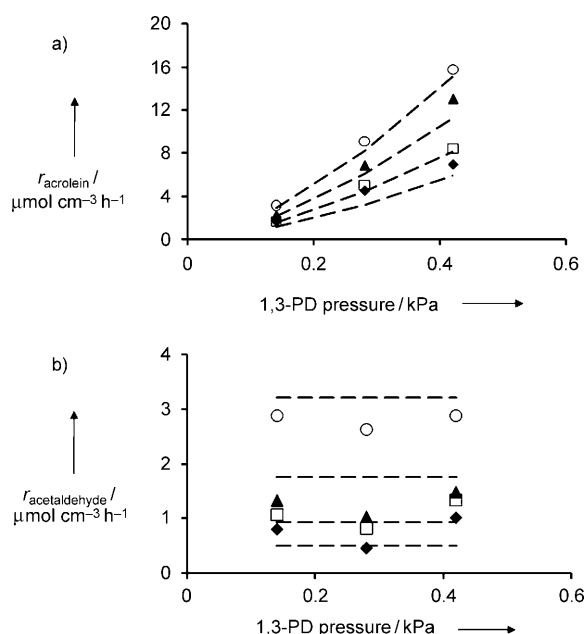


**Figure 3.** Effects of 1,3-propanediol inlet pressure on the formation rate of a) acrolein and b) acetaldehyde [430 K, residence time 12 s, O<sub>2</sub> pressures: 0.25 kPa (◆), 0.47 kPa (◻), 0.89 kPa (▲), 1.62 kPa (○)]. The dashed curves correspond to the functional dependence in Equations (1) and (2).

creasing 1,3-propanediol ( $P_{1,3PD}$ ) and O<sub>2</sub> ( $P_{O_2}$ ) pressures, whereas acetaldehyde formation rates were independent of propanediol pressure and proportional to O<sub>2</sub> inlet pressures:

$$(r_{\text{acrolein}}) = kP_{1,3PD}^{3/2}P_{O_2}^{1/2} \quad (1)$$

$$(r_{\text{acetaldehyde}}) = kP_{O_2} \quad (2)$$

Fractional orders (1.5 in organic substrate; 0.5 in O<sub>2</sub>) for  $r_{\text{acrolein}}$  are typical of free-radical pathways,<sup>[17]</sup> including those initiated by O–O cleavage. Scheme 2 shows several plausible

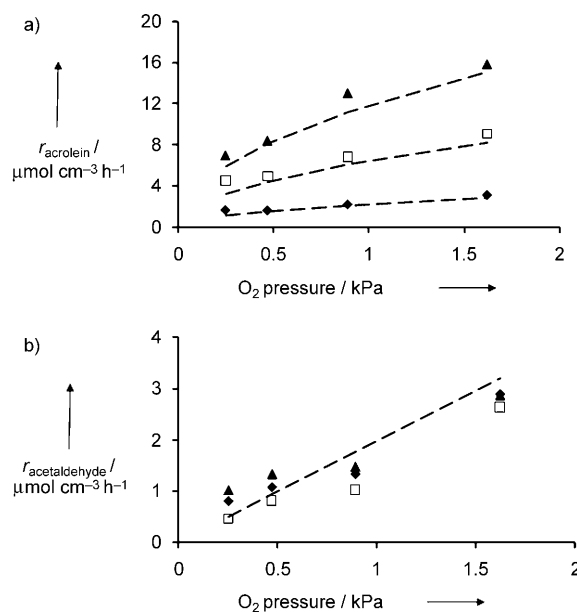
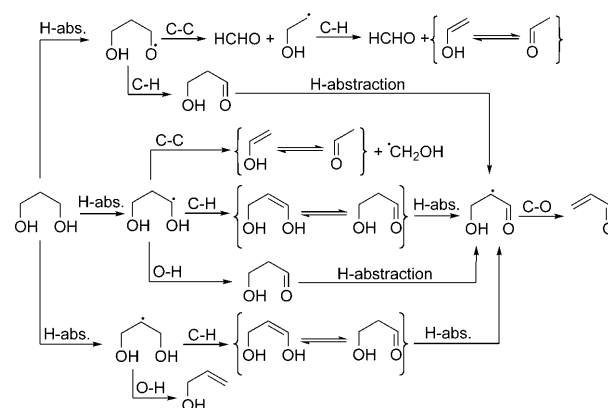


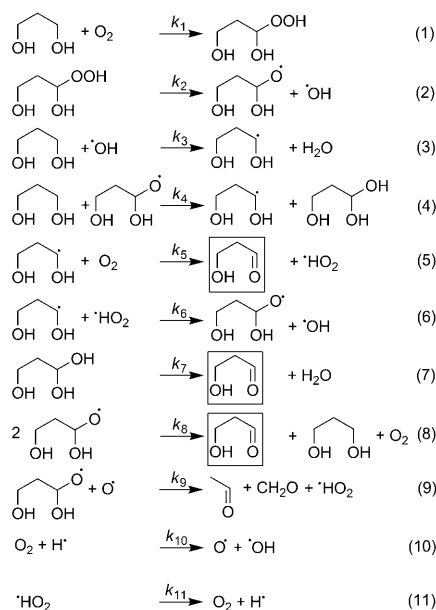
**Figure 4.** Effects of O<sub>2</sub> inlet pressure on the formation rate of a) acrolein, and b) acetaldehyde [430 K, residence time 12 s, diol pressures: 0.14 kPa (◆), 0.28 kPa (◻), 0.42 kPa (▲)]. The dashed curves correspond to the functional dependence in Equations (1) and (2).



**Scheme 2.** Activation pathways for radical-mediated reactions of 1,3-propanediol.

routes for the activation of 1,3-propanediol molecules via H-abstraction pathways. H-abstraction at the  $\alpha$ -position is favored by bond energies.<sup>[18]</sup> The radicals thus formed can then undergo three  $\beta$ -elimination routes to cleave C–C, C–H or O–H bonds. C–C bond cleavage gives acetaldehyde and CH<sub>2</sub>OH•, which then forms formaldehyde and HO<sub>2</sub>• via oxidation.<sup>[19]</sup>  $\beta$ -Elimination with C–H or O–H bond cleavage forms acrolein, but oxygen addition is much faster than this last reaction. O<sub>2</sub> readily adds to  $\alpha$ -hydroxy-alkyl radicals to form  $\alpha$ -hydroperoxyl radicals, which then eliminate HO<sub>2</sub>• to form 3-hydroxypropanal.<sup>[20]</sup> 3-Hydroxypropanal then decomposes rapidly into acrolein via homogeneous pathways.

The elementary reactions proposed in Scheme 3, together with the assumption of pseudo-steady-state for all radical species, leads to an acrolein formation rate equation similar to



**Scheme 3.** 1,3-propanediol oxidation mechanism. The molecules within squares are 3-hydroxypropanal, the fast decomposition of which leads to acrolein

that measured experimentally [Equation (1)]. By analogy with hydrocarbon autoxidation reactions,<sup>[21]</sup> we propose a bimolecular initiation step [Reaction (1)], in which propanediol reacts via O<sub>2</sub> addition into one of its C–H bonds to form hydroperoxide intermediates. The weakest C–H bond in diols is at the α-position,<sup>[21]</sup> and is the C–H bond that is most susceptible to oxygen insertion. The resulting ROOH species then decompose to form •OH and RO• [Reaction (2)],<sup>[22]</sup> which then react via propagation steps that abstract H-atoms from α-carbons in other diol molecules [Reactions (3) and (4)].<sup>[23]</sup> The α-hydroxyalkyl radicals formed in Reactions (3) and (4) can either react with O<sub>2</sub> [Reaction (5)] to form 3-hydroxypropanal and •HO<sub>2</sub> radicals, or with •HO<sub>2</sub> [Reaction (6)] to form RO• and •OH radicals. Reactions (3–6) are bimolecular propagation reactions that consume and form one radical. The unstable 1,1-dihydroxy-3-propanol can undergo intramolecular dehydration to form 3-hydroxypropanal and water [Reaction (7)]. These propagation reactions can terminate via RO• radical recombination to form 3-hydroxypropanal, 1,3-propanediol, and oxygen molecules [Reaction (8)]. It is remarkable that 3-hydroxypropanal is formed—faster than initiation and termination reactions—in a propagation step [Reaction (5)]; this is the cause of the large product formation.

Alternate terminations pathways do not lead to the functional form of the rate data Equation (1) reported here for homogeneous 1,3-propanediol oxidation. The RO• organic radicals formed in Reaction (2) react with O•, yielding acetaldehyde and CH<sub>2</sub>OH•, which decomposes into formaldehyde via subsequent oxidation [Reaction (9)]. By analogy with alkanols, the C–C bond in propanediols are expected to be weaker than the C–H or O–H bonds.<sup>[24]</sup> O• radicals form via Reaction (10), while •HO<sub>2</sub> decomposes into O<sub>2</sub> and H• via Reaction (11).

The pseudosteady-state hypothesis (PSSH) for all intermediates and the long-chain approximation<sup>[25]</sup> lead to an equation for 3-hydroxypropanal formation rates (details in Supporting Information):

$$r_{\text{acrolein}} = r_{3\text{-hydroxypropanal}} = 2k_4 \sqrt{\frac{2k_1}{k_8}} P_{1,3\text{PD}}^{3/2} P_{\text{O}_2}^{1/2} \quad (3)$$

3-Hydroxypropanal was not detected in the effluent stream, because it reacts rapidly via a facile retro-Michael addition to form acrolein.<sup>[26,27]</sup> Thus, acrolein formation rates are also given by Equation (3), in agreement with measured rate data [Equation (1)]. The effective rate constant in Equation (1) is given by the product of a propagation rate constant (*k<sub>4</sub>*) and the square root of the ratio of initiation to termination rate constants (*k<sub>1</sub>*/*k<sub>8</sub>*), as expected for radical-mediated pathways in the limit of long chains.<sup>[25]</sup> The PSSH treatment for the intermediates involved in acetaldehyde formation lead to the rate equation:

$$(r_{\text{acetaldehyde}}) = \frac{k_4 k_{11}}{k_5} P_{\text{O}_2} \quad (4)$$

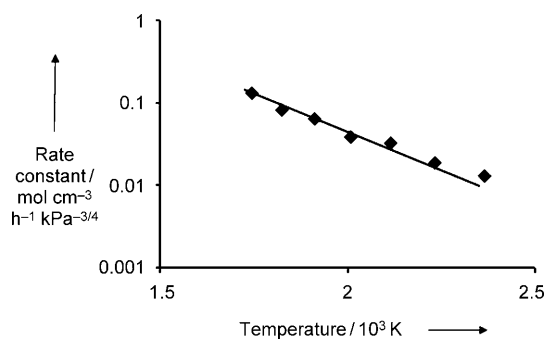
This equation is consistent with the *P<sub>O<sub>2</sub></sub>*

 and *P<sub>13PD</sub>* dependences on acetaldehyde, shown in Figure 3b and 4b and with the stronger effects of O<sub>2</sub> pressure on acetaldehyde formation rates compared with acrolein formation rates.

Equation (3) for acrolein formation rates can be inserted into the design equation for a plug-flow reactor to obtain an equation for the rate constant at each exit conversion (*x<sub>A</sub>*), residence time (*τ*) and temperature (*T*):

$$k = \frac{1}{\tau} \int_0^{x_A} \frac{dx_A}{(1-x_A)^{3/2} (\theta_{\text{O}_2} - 0.5x_A)^{1/2}} \quad (5)$$

in which *θ<sub>O<sub>2</sub></sub>*

 is the inlet O<sub>2</sub>/diol molar ratio. This equation can be used to estimate the rate constant at each temperature (Figure 5) and the apparent activation energy (32+/-2 kJ mol<sup>-1</sup>). This activation energy is lower than the values previously reported of hydrocarbon fuel autoxidations (ca. 150 kJ mol<sup>-1</sup><sup>[28]</sup>), indicating that OH groups in diols increase rate constants for initiation and propagation steps. Homogene-


**Figure 5.** Rate constant for acrolein formation as a function of reciprocal temperature (12.4 s residence time, 0.47 kPa O<sub>2</sub>, 0.28 kPa diol)

ous autoxidation of polypropylene glycol at 348–366 K gave activation energies of ca. 80 kJ mol<sup>-1</sup>.<sup>[29]</sup> These data, taken together with the unreactive nature of propanol and glycerol, indicate a unique effect of the two OH groups in diols on the rates of H-abstraction reactions.

Glycerol can be converted to acrolein and 1-hydroxyacetone on acid catalysts,<sup>[30]</sup> but the homogeneous pathways reported here lead to much higher acrolein yields and selectivities. 1,3-Propanediol may be obtained from glycerol or via fermentation of carbohydrates.<sup>[31]</sup> These high diol conversions and acrolein selectivities lead to acrolein/O<sub>2</sub>/H<sub>2</sub>O streams that may be conveniently introduced into a subsequent catalytic oxidation reactor to give high yields of acrylic acid.

### Coupling homogeneous oxidation of 1,3-propanediol with catalytic conversion of acrolein products to acrylic acid

The acrolein/O<sub>2</sub>/H<sub>2</sub>O mixtures formed via homogeneous oxidation of 1,3-propanediol resemble those used for acrylic acid synthesis on Mo-V oxide catalysts,<sup>[32,33]</sup> and is used here in a tandem reactor strategy to convert diols to acrylic acid without intervening treatment of the effluent between reactors. The homogeneous reactor was fed with a mixture of O<sub>2</sub> (8.8 kPa) and 1,3 propanediol (1 kPa, introduced as 10:1 H<sub>2</sub>O/diol molar ratio) at 503–543 K (14.1 s residence time; 5.6 cm<sup>3</sup> reactor volume). The H<sub>2</sub>O added did not influence homogeneous oxidation rates or selectivities at these conditions (503–543 K, 0.14–0.42 kPa 1,3-propanediol; 0.25–1.62 kPa O<sub>2</sub>). Complete diol conversions were achieved at 543 K (Table 2) and the acrolein yield was 91 %.

**Table 2.** Conversion and carbon selectivity in the homogeneous oxidation of 1,3-propanediol.<sup>[a]</sup>

T [K]	Conversion [%]	Carbon selectivity [%]			
		Acrolein	CH <sub>3</sub> CHO	HCHO	CO <sub>2</sub>
503	75	93	6	0.8	< 0.5
523	85	93	6.5	0.9	< 0.5
543	99.9	91	7.5	0.9	< 0.5

[a] Conditions: 1 kPa 1,3-propanediol, 10 kPa H<sub>2</sub>O, 8.8 kPa O<sub>2</sub>; 14.1 s residence time; 5.6 cm<sup>3</sup> reactor volume.

The effluent from this homogeneous reactor was introduced directly into a subsequent reactor containing Mo<sub>0.61</sub>V<sub>0.19</sub>O<sub>x</sub> catalyst. Figure 6 shows the effects of temperature (513–613 K) in the catalytic reactor on acrolein and acetaldehyde conversions and acrylic acid and acetic acid yields. Acrolein and acetaldehyde conversions increased with reactor temperature and acrylic and acetic acid were the only products detected. This two-step process using sequential homogeneous–heterogeneous reactors produces acrylic acid and acetic acid yields (based on the 1,3-propanediol fed to the homogeneous reactor) of 91 % and 9%, respectively at full conversion of their respective reactants. Acrylic acid formation rates ranged from 0.0017 to 0.0035 mol g<sub>cat</sub><sup>-1</sup> s<sup>-1</sup> at 513 to 613 K reactor temperatures.

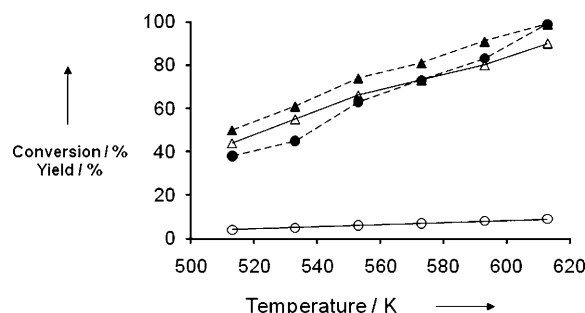


**Figure 6.** Effect of the temperature of the catalytic reactor on acrolein and acetaldehyde conversion, and yields of oxidation products. Feed composition: 1 kPa 1,3-propanediol, 8.8 kPa O<sub>2</sub>, 10 kPa water. Homogeneous reactor: 543 K, residence time 14.1 s. Catalytic reactor: 0.2 g of Mo<sub>0.61</sub>V<sub>0.19</sub>O<sub>x</sub> catalyst, 1.8 g catalyst·(mol 1,3-propanediol)<sup>-1</sup>. Acrolein (▲) and acetaldehyde (●) conversions, acrylic acid (△) and acetic acid (○) yields. Yields were calculated as the percentage of the entering 1,3-propanediol that appears as each product (i.e., acrylic acid and acetic acid).

### Homogeneous 1,2-propanediol oxidation pathways

Homogeneous oxidation of 1,2-propanediol also occurred at conditions similar to described above for 1,3-propanediol conversion. Acetone was the only C<sub>3</sub> product and acetaldehyde, formaldehyde, and CO<sub>2</sub> were also formed via C–C bond cleavage. Acetone selectivities (23–26%) were much smaller than for the C<sub>3</sub> product (acrolein) of 1,3-propanediol oxidation. Product selectivities did not depend on residence time (Table 3), as in the case of 1,3-propanediol, consistent with

**Table 3.** Conversion, reaction rate, and selectivity towards acrolein, acetaldehyde, and formaldehyde in the oxidation of 1,2-propanediol, as a function of residence time.<sup>[a]</sup>

τ [s]	Conversion [%]	-r <sub>1,2PD</sub> [μmol cm <sup>-3</sup> h <sup>-1</sup> ]	Selectivity [%]			
			Acetone	CH <sub>3</sub> CHO	HCHO	CO <sub>2</sub>
11.8	20.1	9.7	23	50	7.6	19.4
8.8	12.5	7.7	26	49	6.2	18.8
7.6	11.6	8.9	25	48	8.4	18.6
6.6	10.3	9.5	25	51	8.3	15.7

[a] Conditions: T = 430 K, 0.28 kPa 1,2-propanediol, 0.89 kPa O<sub>2</sub>.

their direct formation from 1,2-propanediol. Homogeneous oxidation of 1,2-propanediol gave CH<sub>3</sub>CHO/(HCHO+CO<sub>2</sub>) molar ratios near unity, as expected from their concurrent formation via a single C–C bond cleavage of C<sub>3</sub> molecules.

Acetone formation rates increased linearly with increasing diol and O<sub>2</sub> pressures (Figures 7a and 8a), while acetaldehyde formation rates increased with increasing O<sub>2</sub> pressure but decreased as diol pressures increased (Figures 7a and 8a). These acetone formation rate data can be accurately described by the equation:

$$(r_{\text{acetone}}) = kP_{1,2PD}P_{\text{O}_2} \quad (6)$$

Scheme 4 shows a plausible sequence of elementary steps for homogeneous oxidation of 1,2-propanediol. By analogy

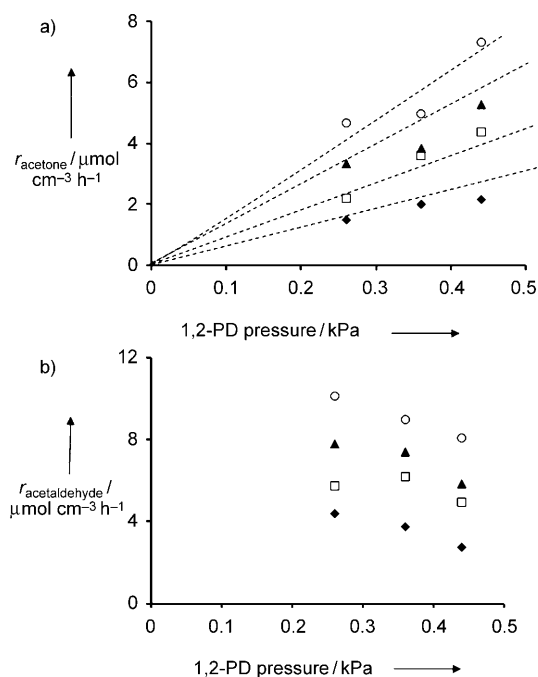


**Figure 7.** Effects of 1,2-propanediol inlet pressure on the formation rate of a) acetone, and b) acetaldehyde [423 K, residence time 12 s, O<sub>2</sub> pressures: 0.25 kPa (◆), 0.47 kPa (◻), 0.89 kPa (▲), 1.62 kPa (○)]. The dashed curves correspond to the functional dependence of acetone in Equation (6).

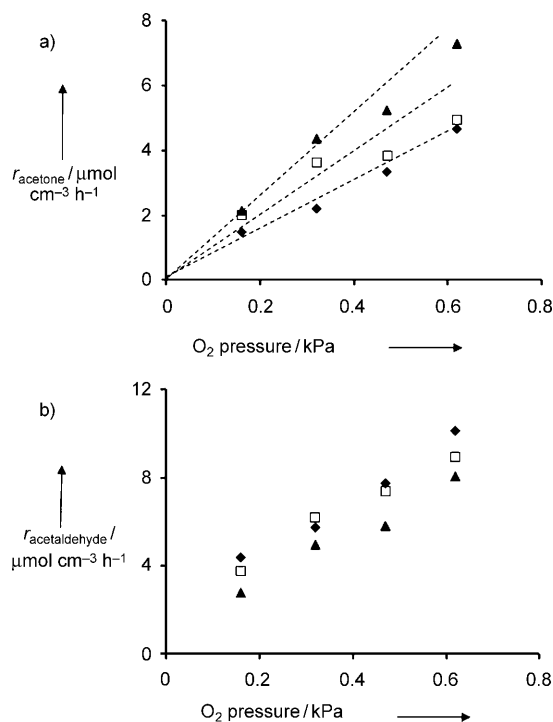
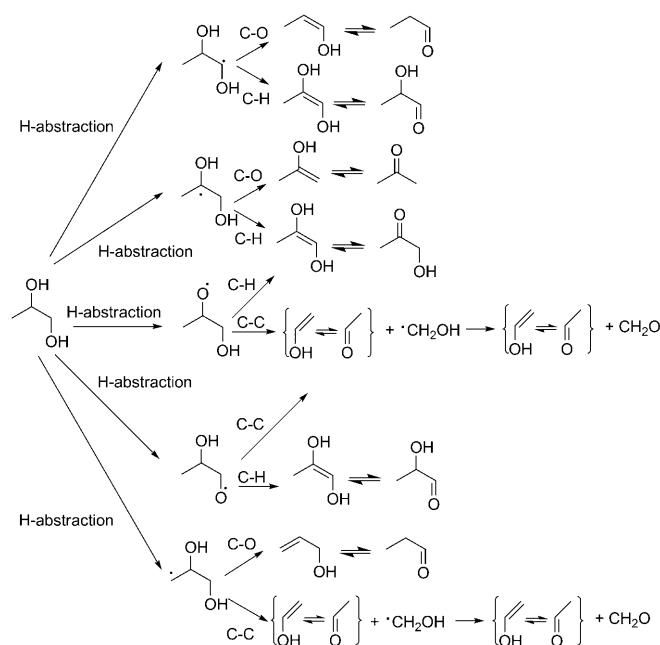


**Figure 8.** Effects of oxygen inlet pressure on the formation rate of a) acetone, and b) acetaldehyde [423 K, residence time 12 s, diol pressures: 0.14 kPa (◆), 0.28 kPa (◻), 0.42 kPa (▲)]. The dashed curves correspond to the functional dependence of acetone in Equation (6).

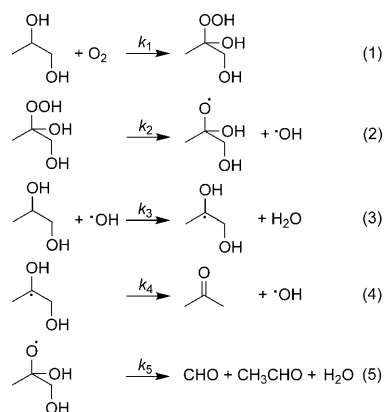
with 1,3-propanediol oxidation, we propose that 1,2-propanediol reacts via O<sub>2</sub> addition at its α- or β-C–H bonds to give the corresponding radicals. β-Elimination reactions can then cleave either C–O or C–H bonds in these radicals. C–O bond cleavage



**Scheme 4.** Plausible reaction routes for 1,2-propanediol.

gives propanal or acetone, depending on the location of the unpaired electron along the C<sub>3</sub> backbone, but propanal was not detected among reaction products. β-Elimination at the C–H bond forms, via addition of oxygen and elimination of ·HO<sub>2</sub>, 2-hydroxy-1-propanal or 1-hydroxy-2-propanone.<sup>[20]</sup>

The elementary reactions proposed in Scheme 5 lead to the measured dependence rate [Equation (6)] for acetone. The pathways for acetone formation reaction involve, as in the case of 1,3-propanediol, bimolecular initiation via O<sub>2</sub> addition, in this case at C–H bonds in either α- or β- positions.<sup>[18]</sup>



**Scheme 5.** Formation of acetone by homogeneous oxidation of 1,2-propanediol.

According to Scheme 4, O<sub>2</sub> addition occurs at β-C–H bonds in 1,2-propanediol to form the intermediate hydroperoxide [Reaction (1), Scheme 5]. This species can then decompose to give OH and organic radicals [Reaction (2)]; the latter propa-

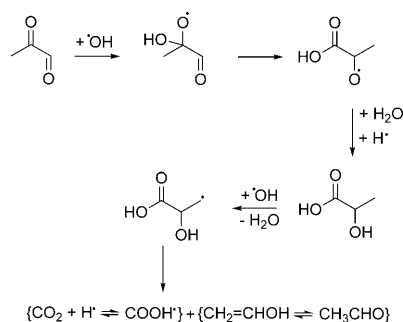
gate chains via H-abstraction from  $\alpha$ - or  $\beta$ -carbons in diols [Reaction (3)]. The hydroxyl-alkyl radicals formed [Reaction (4)] can undergo  $\beta$ -elimination to cleave the C–O bond and form acetone and OH radicals,<sup>[34]</sup> while the oxy-alkyl radicals form acetaldehyde, formaldehyde, and CO<sub>2</sub> in termination steps [Reaction (5)].

The pathways for acetone formation in Scheme 5 and the assumptions of steady-state concentrations for all intermediates in the limit of long radical chains<sup>[25]</sup> lead to an equation consistent with measured rate data (details in Supporting Information):

$$(r_{\text{acetone}}) = \frac{k_1}{2} P_{1,2PD} P_{O_2} \quad (7)$$

in which the rate constant reflects the kinetic constant of oxygen addition to the 1,2-propanediol to form the hydroperoxide.

The low selectivity to acetone (ca. 25%) in homogeneous oxidation of 1,2-propanediol is consistent with the parallel formation of  $\alpha$ - and  $\beta$ -hydroxy-alkyl radicals, in contrast with the nearly exclusive formation of the  $\alpha$ -hydroxy-alkyl radical in 1,3-propanediol reactions, and with the fact that  $\bullet$ OH propagating radicals (but not RO $\bullet$ ) leads to acetone. In Scheme 4, the compounds formed via C–H bond cleavage of  $\alpha$ - and  $\beta$ -hydroxy-alkyl radicals (1-hydroxy-2-propanone and 2-hydroxy-1-propanal) are subsequently oxidized to 2-oxopropanal. This compound reacts (Scheme 6) with  $\bullet$ OH radicals to form a hydroxyacid, which then undergoes H-abstraction and C–C bond cleavage by  $\beta$ -elimination to form 2-hydroxy-1-ol (which forms acetaldehyde via tautomerism) and HO $\dot{C}O$  radicals, which form CO<sub>2</sub> via H-abstraction.<sup>[35]</sup>



**Scheme 6.** Pathways of 2-oxopropanal decomposition.

1,2-Propanediol reacts in presence of oxygen to give acetone, acetaldehyde and formaldehyde as main reaction products (Table 3). Acetone is formed as a product of C–O bond cleavage of  $\beta$ -hydroxy-alkyl radical. Acetaldehyde and formaldehyde are the decomposition products of 2-oxopropanal, which forms via reactions of the C–H bond cleavage products of  $\alpha$  and  $\beta$ -hydroxyl-alkyl radicals. Reaction schemes proposed for both 1,3-propanediol (Scheme 3) and 1,2-propanediol (Scheme 5) are based on radical-like pathways and give rate equations and selectivities consistent with the data reported

here. The symmetry of 1,3-propanediol molecules leads one predominant product (acrolein), while 1,2-propanediol, lacking such symmetry, involve more diverse pathways and oxidation products.

## Conclusions

1,2-Propanediol and 1,3-propanediol react with O<sub>2</sub> at 400–500 K via homogeneous pathways unaffected by catalytic or surface-mediated events. 1,2-Propanediol preferentially reacts via C–C bond cleavage to form CH<sub>3</sub>CHO, HCHO, and CO<sub>2</sub>, with the parallel formation of acetone with modest selectivities. In contrast, 1,3-Propanediol forms acrolein almost exclusively (~90% selectivities and yields) and C–C cleavage products as minority species. These rates and selectivities, as well as the measured dependences of rates on O<sub>2</sub> and 1,3-propanediol pressures are consistent with radical-mediated homogeneous pathways described in the text. High acrolein yields from homogeneous 1,3-propanediol oxidation allow the direct introduction of the reactor effluent into a subsequent catalytic reaction, in which acrolein/H<sub>2</sub>O/O<sub>2</sub> mixtures form acrylic acid with ca. 90% yields based on 1,3-propanediol reactants.

## Experimental Section

The gas-phase oxidation of propanediols was carried out at ambient pressure in a vertical quartz tube (length 50 cm, volume 9 cm<sup>3</sup>), heated resistively and equipped with a concentric axial thermowell and a type-K thermocouple. Quartz granules (1.0–1.5 mm diameter) were used to vary the empty heated volume within the reactor vessel. 1,2-Propanediol or 1,3-propanediol reactants (Aldrich, 99.6%) were introduced as liquids with a syringe pump (Cole Parmer 74900 Series) into a flowing gas stream in a vaporization volume held at 420 K. Helium (Praxair, 99.999%) was used as a diluent and the O<sub>2</sub> co-reactant was introduced as a 10% O<sub>2</sub>/He mixture, (Praxair). Molar rates were metered by electronic controllers (Bronkhorst) and all transfer lines were kept at 420 K to prevent condensation. Temperatures (400–600 K), flow rates (1.4 × 10<sup>-4</sup>–8.3 × 10<sup>-4</sup> mol diol h<sup>-1</sup>), and O<sub>2</sub>/diol ratios (0–3.2) were varied systematically throughout these experiments.

Reactants and products were analyzed by gas chromatography (Hewlett–Packard 5890) using a Carboxen-1000 column (60–80 mesh, 5.22 m × 3.18 mm) with thermal conductivity detection and a methyl silicone capillary column (HP-1; 50 m × 0.32 mm, 1  $\mu$ m film) with flame ionization detection. The identity of reaction products was determined from the elution time of known compounds and their speciation was confirmed by mass spectrometry (HP-6890/5973, 50 m HP-1 column). Diol conversions are reported as the percentage of the entering reactants converted to products. Selectivities are reported on a carbon basis as the percentage of the converted diol reactants appearing as each product. Residence time is defined as the ratio of the reactor volume to the inlet volumetric rate at standard conditions (STP). Carbon balances were > 95% in all experiments. The presence of organic peroxides in diol reactants was ruled out for both 1,2- and 1,3-propanediol reactants by using Whatman indicators (< 10 ppm). Peroxides were not detected in either reactant, indicating that the observed homogeneous reactions are not initiated by adventitious peroxide impurities.

A Mo-V oxide ( $\text{Mo}_{0.61}\text{V}_{0.19}\text{O}_x$ ) catalyst<sup>[34]</sup> was used to convert acrolein, present in the effluent from the homogeneous 1,3-propanediol oxidation reactor, into acrylic acid; this catalyst also converts acetaldehyde to acetic acid. The catalyst was prepared by mixing a solution containing  $\text{C}_2\text{O}_4\text{H}_2$  (Fluka, 99%) and  $\text{NH}_4\text{VO}_3$  (Sigma-Aldrich, 99%) in deionized water with one containing  $(\text{NH}_4)_6\text{Mo}_7\text{O}_{24}\cdot 4\text{H}_2\text{O}$  (Aldrich, 99.98%) at ambient temperature. The liquid was evaporated at 363 K while stirring and the residual solids were treated at 393 K in ambient air overnight and then in flowing dry air at 673 K for 4 h (Praxair, extra dry).

Acrolein oxidation was carried out in a tubular packed bed reactor with plug-flow hydrodynamics placed after the homogeneous reactor. The reactor contained  $\text{Mo}_{0.61}\text{V}_{0.19}\text{O}_x$  (0.2 g) diluted with acid-washed quartz powder (1 g) to prevent temperature gradients. The homogeneous reactor was fed with a mixture containing 1,3-propanediol (1 kPa),  $\text{O}_2$  (8.8 kPa), and  $\text{H}_2\text{O}$  (10 kPa) at 543 K and 14.1 s residence time. Complete conversion of 1,3-propanediol was reached in the first reactor, with selectivities of 91%, 7.5%, and 0.9% for acrolein, acetaldehyde, and formaldehyde. This stream was then introduced into the catalytic reactor described above. Reactant and product concentrations were measured by gas chromatography using the same procedures as for the homogeneous reactor.

## Acknowledgements

Prof. W. H. Green (Massachusetts Institute of Technology) and Prof. S. Ordóñez (University of Oviedo) are acknowledged for their helpful mechanistic discussions. E.D. acknowledges financial support from the Spanish Ministry of Science and Innovation (José Castillejo Program). This work was supported by BP as part of the Methane Conversion Cooperative at the University of California at Berkeley and by the Director, Office of Basic Energy Sciences, Chemical Sciences Division, US Department of Energy under contract DE-AC02-05CH11231.

**Keywords:** diols · oxidation · radicals · reaction mechanisms · sustainable chemistry

- [1] G. W. Huber, J. N. Chheda, C. J. Barrett, J. A. Dumesic, *Science* **2005**, *308*, 1446–1450.  
 [2] G. W. Huber, S. Iborra, A. Corma, *Chem. Rev.* **2006**, *106*, 4044–4098.  
 [3] A. Corma, S. Iborra, A. Velty, *Chem. Rev.* **2007**, *107*, 2411–2502.  
 [4] M. Pagliaro, R. Ciriminna, H. Kimura, M. Rossi, C. D. Pina, *Angew. Chem.* **2007**, *119*, 4516–4522; *Angew. Chem. Int. Ed.* **2007**, *46*, 4434–4440.

- [5] A. Corma, G. W. Huber, L. Sauvanaud, P. O'Connor, *J. Catal.* **2008**, *257*, 163–171.  
 [6] G. Knothe, J. Krahl, J. V. Gerpen, *The Biodiesel Handbook*, AOCS, Champaign **2005**.  
 [7] G. A. Kraus, *Clean: Soil, Air, Water* **2008**, *36*, 648–651.  
 [8] G. Chuchani, R. M. Dominguez, A. Rotinov. I. Martin, *Int. J. Chem. Kinet.* **1997**, *29*, 851–854.  
 [9] J. Shen, W. Shan, Y. Zhang, J. Du, H. Xu, K. Fan, W. Shen, Y. Tang, *Chem. Commun.* **2004**, 2880–2881.  
 [10] J. Shen, W. Shan, Y. Zhang, J. Du, H. Xu, K. Fan, W. Shen, Y. Tang, *J. Catal.* **2006**, *237*, 94–101.  
 [11] E. Sokolova, *Electrochim. Acta* **1979**, *24*, 147–155.  
 [12] H. Huser, J. M. Leger, C. Lamy, *Electrochim. Acta* **1985**, *30*, 1409–1414.  
 [13] C. Alonso, J. González-Velasco, *J. Appl. Electrochem.* **1988**, *18*, 538–545.  
 [14] L. Giebeler, P. Kampeb, A. Wirth, A. H. Adamsa, J. Kunert, H. Fuess, H. Vogel, *J. Mol. Catal. A: Chem.* **2006**, *259*, 309–318.  
 [15] Z. R. Ismagilov, S. N. Pak, V. K. Ermoleav, *J. Catal.* **1992**, *136*, 197–201.  
 [16] F. Wang, J.-L. Dubois, W. Ueda, *J. Catal.* **2009**, *268*, 260–267.  
 [17] J. I. Steinfeld, J. S. Francisco, W. L. Hase, *Chemical Kinetics and Dynamics*, 2<sup>nd</sup> Ed., Prentice-Hall, New Jersey **1999**.  
 [18] S. R. Logan, *Can. J. Chem.* **1991**, *69*, 540–544.  
 [19] N. I. Butkovskaya, N. Pouvesle, A. Kukui, Y. J. Mu, G. Le Bras, *J. Phys. Chem. A* **2006**, *110*, 6833–6843.  
 [20] I. Hermans, T. L. Nguyen, P. A. Jacobs, J. Peeters, *ChemPhysChem* **2005**, *6*, 637–645.  
 [21] A. G. Davies, *Organic Peroxides*, Butterworth, London **1961**.  
 [22] V. Warth, F. Battin-Leclerc, R. Fournet, P. A. Glaude, G. M. Come, G. Scacchi, *Comput. Chem.* **2000**, *24*, 541–560.  
 [23] C. F. Cullis, E. A. Warwicker, *Proc. R. Soc. London Ser. A*, **1961**, *264*, 392–407.  
 [24] Y.-R. Luo, *Handbook of Bond Dissociation Energies in Organic Compounds*, CRC Press, Boca Raton **2003**.  
 [25] M. Boudart, *Kinetics of Chemical Processes*, Prentice-Hall, New Jersey **1968**.  
 [26] L. H. Slaugh, J. P. Arhancet (Shell Oil Company), US 5304686, **1994**.  
 [27] E. Tsukuda, S. Sato, R. Takahashi, T. Sodesawa, *Catal. Commun.* **2007**, *8*, 1349–1353.  
 [28] J. M. Pickard, E. G. Jones, *Energy Fuels* **1996**, *10*, 1074–1077.  
 [29] M. A. Semsarzadeh, H. Salehi, *Eur. Polym. J.* **2000**, *36*, 1001–1010.  
 [30] A. Neher, T. Haas, D. Arntz, H. Klenk, W. Girke (Degussa Aktiengesellschaft), US 5387720, **1995**.  
 [31] D. M. Adkesson et al. (E. E. Dupont de Nemours and Company and A. E. Staley Manufacturing Company), WO 101479, **2004**.  
 [32] T. V. Andrushkevich, G. Ya Popova, *Russ. Chem. Rev.* **1991**, *60*, 1023–1034.  
 [33] J. Tichý, *Appl. Catal. A: Gen.* **1997**, *157*, 363–385.  
 [34] R. Janik, W. Gerhardt, *J. Prakt. Chemie (Leipzig)* **1989**, *331*, 611–616.  
 [35] S. Yamabe, N. Tsuchida, S. Yamazaki, *J. Org. Chem.* **2006**, *71*, 1777–1783.  
 [36] X. Li, E. Iglesia, *Appl. Catal. A: Gen.* **2008**, *334*, 339–347.

Received: May 19, 2010

Revised: June 20, 2010

Published online on September 9, 2010